**Journal of Physical Chemistry and Functional Materials**

Home Page of Journal: https://dergipark.org.tr/jphcfum


# Inhibition of Aluminium Alloy Corrosion by Thiourea and Lithium ion in 3.5 % NaCl Solution Using Gravimetric, Adsorption and Theoretical Studies

*Anderson Umezurike. Ezeibe*[a], *Emmanuel Chile Nleonua,*[b]*, *Chika Cecelia. Unegbu*[a] *and Ilham Ben Amor*[c]

[a]*Department of Chemistry, Federal Polytechnic Nekede, P.M.B. 1036 Owerri, Imo State, Nigeria*
[b]*Materials and Electrochemical Research Unit (MERU), Federal Polytechnic Nekede, P.M.B. 1036 Owerri, Imo State, Nigeria*
[c]*Department of Process Engineering and Petrochemical, Faculty of Technology, University of El Oued, El Oued 39000, Algeria*
**Corresponding author: E-mail: enleonu@yahoo.com*

**ABSTRACT**

The adsorption and inhibition performance of thiourea and lithium ion on aluminium corrosion in 3.5 % NaCl were investigated using gravimetric measurement, scanning electron microscope (SEM) analysis and quantum chemical computational techniques respectively. Gravimetric analysis revealed that thiourea has a good inhibitory efficacy of 82 % at 1 mM concentration of thiourea on the corrosion inhibition of aluminum under the conditions studied. Also, poor inhibitory effects were recorded with an increase in the concentration of inhibitor, and improvement in inhibition efficiency was observed with the addition of lithium ion. In addition, the effects of temperature (303–333 K) on corrosion inhibition was investigated. The findings showed that the effectiveness of the inhibition rises with temperature. The adsorption of thiourea molecules onto an aluminium surface followed the Temkin adsorption isotherm, while the mixed inhibitor of thiourea and lithium ion followed the Langmuir adsorption isotherm model. SEM results confirmed that the inhibition mechanism is due to the formation of a protective thin film on the aluminium surfaces that prevents corrosion. Quantum chemical calculations based on the density functional theory (DFT) revealed that the presence of sulphur and nitrogen in the structure of thiourea molecules is responsible for the strong inhibitory performance due to possible adsorption with Al atoms on the metal surface. The computed experimental and theoretical parameters in this investigation are in good agreement.

**ARTICLE INFO**

*Keywords*:

Corrosion inhibition
Gravimetric analysis
Thiourea
Lithium ion
Synergistic effect
Density functional theory

**Received**: 2022-11-02
**Accepted**: 2022-11-27
**ISSN**: 2651-3080
**DOI:** 10.54565/jphcfum.1198578

## Introduction

Aluminium is considered to be one of the most important non-ferrous metals used in engineering applications [1]. The continuous growth of aluminium consumption, especially in many industrial applications such as machine tools and parts, fittings, nuts and bolts, cooking pots, plates, reaction tanks and storage tanks, is due to its promising characteristics such as low density, ease of recycling, diversity of its alloy, high strength to weight ratio, good machining performance, excellent electrical and thermal conductivity [2]. The characteristic properties of aluminium and its alloys have made them an ideal engineering material for substituting heavier materials such as copper and iron within the transportation industry in response to weight reduction demand [3]. Despite all these excellent characteristics and features possessed by aluminum, one of the greatest challenges to the use of aluminium in industrial application is its susceptibility to corrosion attack [4,5]. Aluminum is a passive metal in the presence of atmospheric air and neutral aqueous solutions, but excessive corrosion attack is known to occur on aluminum surfaces in chloride solutions from various sources of corrosive media [6]. Aluminium suffers corrosion at its early stage with gradual deterioration during use, and the rate of corrosion differs from one aluminum alloy to another depending on their microstructure composition. As a result, aluminum corrosion control becomes a critical issue in terms of environmental protection, human safety, cost savings, and material loss [5].

Presently, the corrosion inhibition of aluminium and its alloys is a major area of concern to researchers because of its tremendous importance in industrial applications [7]. Chromate compounds are still the best and most effective corrosion inhibitors but are being limited due to their environmental problems, toxicity and carcinogenicity [8,9]. Most of the commercial inhibitors are toxic in nature. Therefore, replacement by environmentally friendly inhibitors is important [10]. Over the years, extensive research has been conducted to find an alternative new range of inhibitor compounds with desirable attributes such as being non-toxic and readily available. Organic compounds have been potential materials for the surface protection of ferrous and non-ferrous metals and their alloys against aggressive environments [6,11]. The performance of organic molecules utilized as corrosion inhibitors produces coordination complexes with the metallic surface utilizing the active sites, and these complexes occupy a significant surface area, thereby coating the metallic surface and shielding it from corrosive solutions [12].

Recently, researchers are paying more attention to mixed inhibitors because of their synergistic effects. Researchers have found that mixtures of inhibitor molecules and other additives enhance corrosion inhibition efficiency more than individual members [13], mainly due to the inherent synergistic corrosion inhibition effect between anions and cations [14]. On this basis, many additives have been used to improve the inhibition efficiency of organic and inorganic inhibitors. The objective of this current study is to evaluate the synergistic effect of $Li^+$ ion and thiourea as corrosion inhibitor components for aluminum in 3.5 % NaCl solution. Gravimetric techniques, morphological analysis, thermodynamics, and adsorption isotherm models were used to explore the anti-corrosion performance of the inhibitors. In addition, density functional theory (DFT) and molecular dynamics (MD) simulation were further employed to provide theoretical insights into the inhibition mechanism. The molecular structure of the inhibitor utilized in this study is shown in Figure 1.

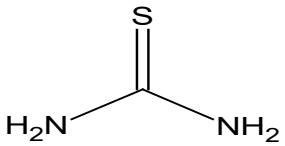


**Figure 1.** Molecular structure of thiourea

## Materials and Methods

### Materials Preparation

The corrosive environment in this investigation was 3.5 % sodium chloride (NaCl) solution which was made from an analytical grade (BDH) of NaCl and deionized water. Thiourea and Lithium chloride were products of BDH having 98 % purity. These chemicals were used without further purification. Aluminium sheet used for the study has the following chemical composition (Wt%): Al(99.19), Si(0.23), Fe(0.44), Cu(0.021), K(0.03), Mg(0.019), Cr(0.0041), Ni(0.005), Mn(0.065), Aluminium coupons with dimensions 2 × 2 × 0.5 cm were applied. The coupons were polished several times with fine emery paper of 1200 grade. The aluminium coupons were degreased with acetone, rinsed with deionized water, dried with warm air and stored in a desiccator before being used for corrosion studies. The inhibitor concentration used was in the range of 1 mM to 5 mM of thiourea. For synergistic effect, 0.05 M of lithium ion with thiourea concentrations of 1 mM, 2 mM, and 4 mM, respectively were used.

Weight Loss Measurements

The corrosion rate measurements were conducted in the environment of 3.5 % NaCl by complete immersion of aluminium coupons with a total surface area of 12 $cm^3$. Each test was conducted in a 250 ml glass beaker having 100 ml of 3.5 % NaCl as a corrosive environment in the absence and presence of the tested corrosion inhibitor. A clean aluminium coupon was weighed and exposed to corrosive solution. After 24 hr, 48 hr, 72 hr, 96 hr, and 120 hr of exposure in 3.5 % NaCl solution in the absence and presence of thiourea at various concentrations (1,2,3, 4, and 5 mM), the coupons were retrieved. The coupon was washed with deionised water, rinsed with acetone, dried with warm air and weighed on an electronic balance. The experiments were conducted in triplicates. From the weight loss measurement data, corrosion rate (CR, $mmy^{-1}$), degree of surface coverage (θ) and inhibition efficiency (1E %), were determined using equations (1) to (3), respectively.

$$C_R = \frac{\Delta W}{DAT} \quad (1)$$

$$\theta = 1 - \frac{C_{Rinh}}{C_{Rblank}} \quad (2)$$

$$IE\ (\%) = \left[1 - \frac{C_{Rinh}}{C_{Rblank}}\right] \times 100 \quad (3)$$

Where $C_R$ is the corrosion rate, W is the weight loss, D is the density of the coupon, A is the surface area of the coupon, and T is the immersion time of the coupon in the corrosive environment. $C_{Rinh}$ and $C_{Rblank}$ are the corrosion rates in the presence and absence of the inhibitor in a 3.5 % NaCl solution.

**Effect of Temperature**

The analysis of aluminium coupons corrosion rate on the variation of temperature was investigated at 303, 313, 323 and 333 k respectively by equilibrating the beaker in a thermostatic water bath (SHZ-88 Model). A clean coupon was weighed and exposed to the corrosive solution. The coupons were retrieved after 1h of exposure time in a 3.5 % NaCl solution in the absence and presence of tested inhibitors at 1 mM concentration and different investigated temperatures. The retrieved coupons were washed with deionized water, rinsed with acetone, dried with warm air and weighed.

Synergistic Effect

The synergistic effect on the corrosion rate of aluminium coupons was investigated for the inhibited solution. Each aluminium coupon was immersed in 100 ml of 3.5 % NaCl solution containing thiourea (1 mM, 2, 4 mM) and 0.05 M lithium ion. Also, the temperature variation effect was monitored at different temperatures of 303–333 K containing 0.3 mM thiourea and 0.05 M lithium ion. The coupons were withdrawn after a 1 h interval up to a maximum time of 5 h.

The withdrawn coupons were washed with deionized water, rinsed with acetone, dried with warm air and weighed.

**Quantum Chemical Computational Studies**

The quantum chemical calculations were performed in order to study the effect of the thiourea structure on the inhibition efficiency. The theoretical calculations were performed using the density functional theory (DFT) with B3YLP: 6-31G functional and DND as the basis set programs in DMOl3 as contained in the material studio software version 7.0 (Biovia, Accelrys). The thiourea structure, electron density, highest occupied molecular orbital (HOMO), lowest unoccupied molecular orbital (LUMO), and physical properties were all completely optimized geometrically. The HOMO, LUMO, global hardness ($\eta$), global softness (σ), electro negativity (χ), ionization energy (I), electron affinity (A), energy gap (ΔE) and fraction of electron transferred (ΔN) were calculated using equation (4) – (11) [15,16].

$$\Delta E = E_{LUMO} - E_{HOMO} \quad (4)$$

$$\eta = -\frac{E_{HOMO} - E_{LUMO}}{2} \quad (5)$$

$$6 = \frac{1}{\eta} \quad (6)$$

$$\mathrm{I} = -E_{LUMO} \quad (7)$$

$$\mathrm{A} = -E_{HOMO} \quad (8)$$

$$\chi = -\frac{\mathrm{E_{HOMO}} + E_{LUMO}}{2} \quad (9)$$

$$\Delta \mathrm{N} = \frac{\chi_{Al} - X_{inh}}{2(\eta_{Al} + \eta_{inh})} \quad (10)$$

$$\omega = \frac{x^2}{2\eta} \quad (11)$$

Where $\chi_{Al}$ = 5.6 eV and $\chi_{inh}$ represents the absolute electronegativity of aluminium and thiourea respectively. $\eta_{A1}$ = 0 and $\eta_{inh}$ represent the absolute global hardness of aluminium and thiourea molecule respectively.

**Molecular Dynamics Simulation**

Molecular Dynamics (MD) simulation were carried out at a molecular level using forcite quench dynamics in the material studio 7.0 software (Accelrys, inc). The Al crystal was cleaved along A1 (110) being the most stable and also the most densely packed when compared to other types of A1 surfaces [17]. Forcite quench molecular dynamics was applied to determine the low energy configurations of adsorbed thiourea molecules on the A1(110) surface. Computation was performed in a 5 x 4 super cell with a 30 Å vacuum plate at 350 k in 5000 steps and simulation time of 5 ps. The COMPASS (Condensed-phase optimized molecular potentials for atomistic simulation studies) force field was used to optimize the entire system.

**Toxicity Prediction of Inhibitor**

The toxicity and physical characteristics of thiourea were predicted using ADMETsar server version 2 based on the relationship between the quantitative structure and activity of the molecular structure of the inhibitor.

**Results and Discussion**

**3Gravimetric Loss Measurement Result**

A Non-electrochemical method like weight loss measurement was used in this study due to its availability, simplicity, and reliability of measurement. Gravimetric measurement techniques provide a suitable method for monitoring metal corrosion and inhibition immersion tests within a long-term because it gives a direct result on the visual and physical effect of corrosion with regards to a metal loss at the corrodent metal interphase in the presence or absence of inhibitor [5]. The corrosion rate of aluminium coupons in inhibited and blank 3.5 % NaCl solutions was determined through weight loss techniques at various concentrations of thiourea after immersion periods (24, 48, 72, 96, 120 h) at 303 K. The experimental results are presented in Figure 2. Careful observation of the percentage inhibition efficiency showed gradual increase in inhibition efficiency of thiourea on the aluminium coupon except at inhibitor concentrations of 5 mM which shows 42 % inhibition efficiency. The low inhibition efficiency observed in the commencement of reaction with 1-4 mM thiourea could be attributed to a time interval needed by the inhibitor to become adsorbed on the aluminium surface. At a concentration of 1 mM, the inhibition efficiency increased from 10 to 82 % when the exposure period increased from 24 to 120 h. Furthermore, the inhibition efficiency from 2 to 5 mM increased from 24 to 72 h, and after 72 h, the inhibition efficiency decreases. Thus, decreased inhibition efficiency suggests an unfavorable interaction at the interphase between thiourea molecules and the aluminium surface resulting from an increase in inhibitor concentration and can be attributed to unstable adsorption. A similar observation has been made by earlier researchers. They observed that thiourea has high inhibition efficiency at low concentrations and loses its inhibition performance at higher concentrations. The attributed low inhibition efficiency of thiourea is caused by its protonated species, which is controlled by the charge density on the sulphur atom, the weakening of the C-S bond and the reactivity of the molecule [18].

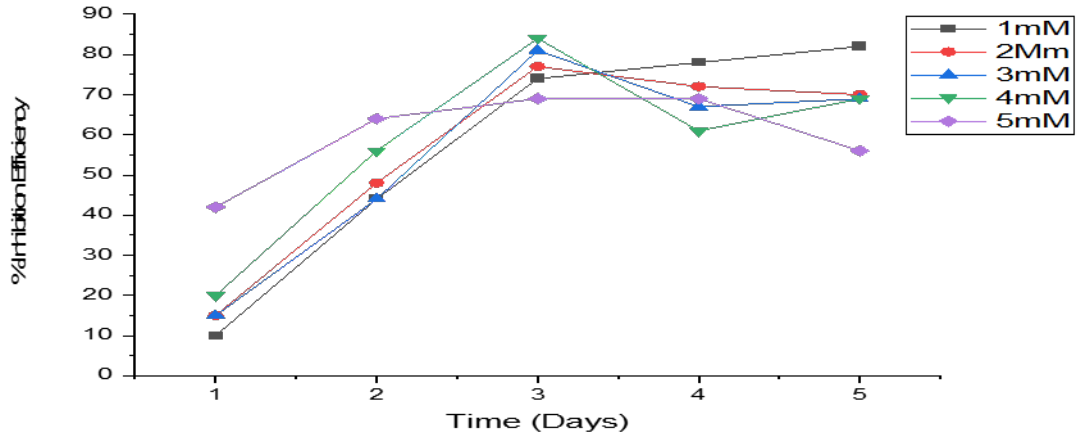


**Figure 2.** Difference of inhibition efficiency in 3.5 % NaCl on the surface of aluminum at various exposure time in the presence of thiourea.

**Effect of Temperature**

Temperature was used to monitor the interaction between the aluminium surface and the corrosive environment in the absence and presence of a tested inhibitor (thiourea). Figure 3 depicts the inhibition efficiency values obtained from weight loss measurements for aluminum coupons in 3.5 % Nacl in the presence of 1 mM thiourea at temperatures ranging from 303 to 333 K. The inhibition efficiency result shows that the percentage inhibition performance increased with raising the temperature of the system in the presence of the inhibitor for 1hr immersion time. The increases in inhibition efficiency may be due to increases in the number of active sites available for adsorption of inhibitor molecules caused by increases in temperature [10]. Hence, thiourea works as an effective inhibitor in the range of temperatures studied at the inhibition concentration of 1 mM.

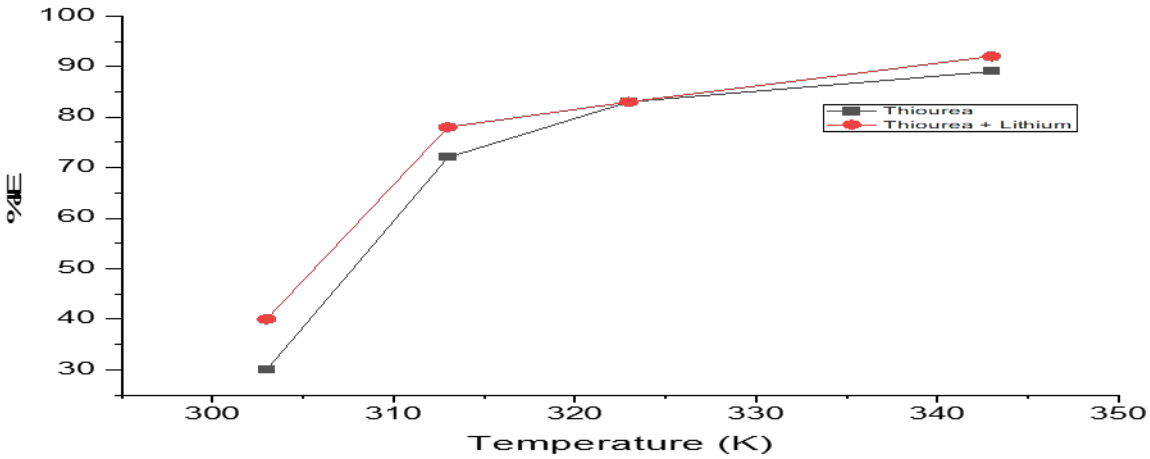


**Figure 3.** Difference of inhibition efficiency in 3.5 % NaCl on the surface of aluminum at various temperature in the presence of thiourea, thiourea and lithium ion.

**Synergistic Effect to Inhibition Efficiency**

To further reorganize the adsorption behavior of inhibitor molecules on the aluminium surface, a synergistic corrosion inhibition effect between lithium ion and thiourea was studied with thiourea concentrations of 1, 2, and 4 mM with 0.05 M of $Li^+$ at 303 K. Based on Figure 4, the combination of lithium ion and thiourea in the 3.5 % NaCl medium improves the percentage inhibitory efficiency. The efficacy of the mixed inhibitors decreases with an increase in the concentration of thiourea inhibitor after 72 hr of immersion time. The presence of lithium ion in the corrosive media increases the inhibition efficiency of the inhibitors when compared to the inhibition efficiency of thiourea, which occurs only in the corrosive media. This is because the mixed inhibitors in the corrosive medium are able to protect the aluminium coupon by forming a protective layer on the surface.

As shown in Figure 3, the inhibition efficiency of thiourea and lithium-ion mixture shows a better mechanism in protecting the aluminium surface at different studied temperatures. The inhibition efficiency is directly proportional to temperature as the higher the temperature, the higher the percentage inhibition efficiency. This indicates a slowing down of corrosion rate due to an increase in the adsorption of inhibitor molecules on the number of exposed active sites [10].

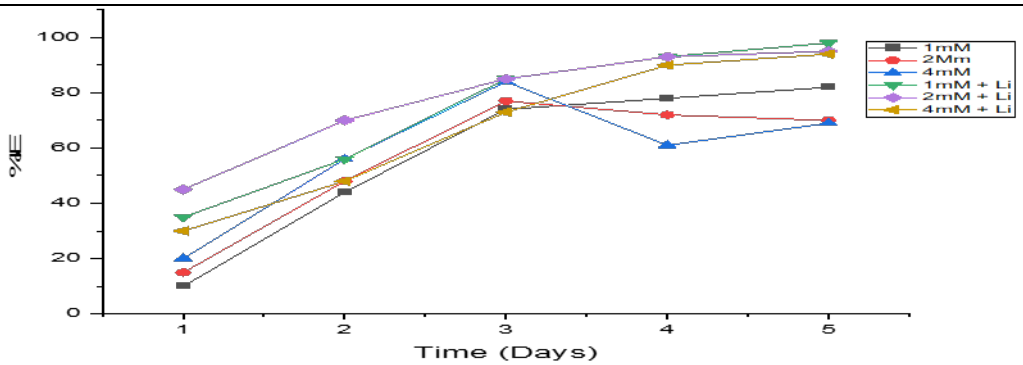


**Figure 4.** Difference of inhibition efficiency in 3.5 % NaCl on the surface of aluminium at various exposure time in the presence of thiourea and lithium ion.

**Adsorption Isotherm**

Thiourea and thiourea with a combination of lithium ion were exploited for the purpose of reducing the corrosion rate in the corrosive solution due to the adsorption of these inhibitor molecules on the surface of the test metal. The adsorption depends on the chemical structure of the inhibitor, the stable conformation in the solution, the surface of the tested metal, and the solution temperature [19]. To further cognize the adsorption behavior of inhibitor molecules on the aluminium surface, different adsorption isotherms, namely, Flory-Huggins, Frumkin, Freundlich, Langmuir, and Temkin, were applied to the tested inhibitor on the surface of the aluminium coupon in the 3.5 % NaCl solution. The correlation coefficient ($R^2$) was used to evaluate the better fit that describes the adsorption mechanisms [20].

$$lnC_{inh}\left(\frac{\theta}{1-\theta}\right) = lnK_{ads} + 2d\theta \quad \text{(Frumkin)} \quad (12)$$

$$log\ \frac{\theta}{C} = logK_{ads} + xlog(1-\theta) \quad \text{(Flory-Huggins)} \quad (13)$$

$$\log\theta = logK_{ads} + nlogC \quad \text{(Freundlich)} \quad (14)$$

$$\frac{C}{\theta} = \frac{1}{K_{ads}} + C \quad \text{(Langmuir)} \quad (15)$$

$$-2a\theta = (lnK_{ads} + lnC) \quad \text{(Temkin)} \quad (16)$$

Where C is the concentration of inhibitor, $K_{ads}$ represents the adsorption equilibrium constant and θ denotes the surface coverage obtained from the gravimetric measurement. The relationship between the degree of surface coverage and inhibitor concentration for the above-mentioned adsorption isotherms was plotted and the values for the adsorption isotherm parameters obtained are presented in Table 1.

It was found that adsorption of thiourea molecules on an aluminium surface in 3.5 % NaCl solution followed the Temkin adsorption isotherm (as shown in Figure 5) because its coefficient of linear correlation ($R^2$) (0.9622) is closer to unity than other studied isotherms. The adsorption equilibrium constant ($K_{ads}$) shows the strength of adsorption of the inhibitor molecules on the surface of the aluminium coupon. The values of $K_{ads}$ of thiourea inhibitor from the Temkin isotherm are in better agreement with the experimental findings compared to $K_{ads}$ values from other isotherms.

It is seen from Table 1 that adsorption of thiourea in combination with lithium ion on an aluminium surface followed the Langmuir adsorption isotherm as 0.9999 was obtained as its coefficient of linear correlation ($R^2$), which was closer to unity than other isotherms (Figure 6). The adsorption study of synergistic effects shows that the value of $K_{ads}$ from the Frumkin isotherm is in better agreement with the experimental data compared to the $K_{ads}$ value of the Langmuir isotherm. The behavior may be attributed to interaction between the aluminium surface and adsorbed inhibitor species and changes in the heat of adsorption with an increase in the degree of surface coverage. The deviation of $K_{ads}$ in the synergistic effect of lithium thiourea inhibitor on the adsorption isotherm implies that the Langmuir isotherm could not be applied in the adsorption mechanism because it indicates some form of divergence from the monolayer adsorption mechanism [21].

**Table 1:** Calculated values of adsorption isotherm parameters for Frumkin, Flory-Huggins, Freundlich, Langmuir and Temkin isotherms in the presence of thiourea.

| Adsorption Isotherm | Intercept | $K_{ads}$ | slope | $R^2$ |
|---|---|---|---|---|
| Temkin | 0.1252 | 0.8889 | 0.4705 | 0.9622 |
| Freundlich | -1.9292 | 0.1453 | 0.7883 | 0.2363 |
| Flory-Huggins | -0.4314 | 0.3703 | -0.0519 | 0.1814 |
| Langmuir | 9.6521 | 0.1036 | -1.0239 | 0.5181 |
| Frumkin | -1.8066 | 0.1642 | 8.6678 | 0.7502 |

**Table 2:** Calculated values of adsorption isotherm parameters for Frumkin, Flory-Huggins, Freundlich, Langmuir and Temkin isotherms in the presence of thiourea and lithium ion.

| Adsorption Isotherm | Intercept | $K_{ads}$ | Slope | $R^2$ |
|---|---|---|---|---|
| Temkin | 0.9766 | 1.7517 | -0.287 | 0.9209 |
| Freundlich | -0.1730 | 0.841 | 0.1004 | 0.6929 |
| Flory-Huggins | -1.9025 | 0.0125 | -1.125 | 0.8710 |
| Langmuir | -0.055 | -18.1818 | 1.0793 | 0.9999 |

| | | | | |
|---|---|---|---|---|
| Frumkin | 6.6496 | 772.47 | - 2.8846 | 0.0577 |

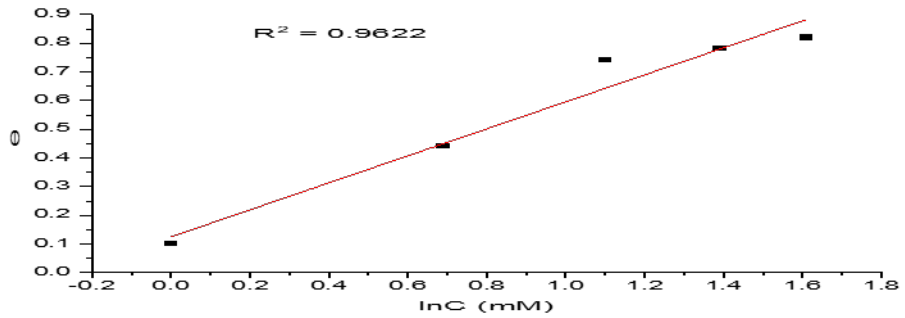


**Figure 5.** Temkin isotherm plot for the adsorption of thiourea on aluminium

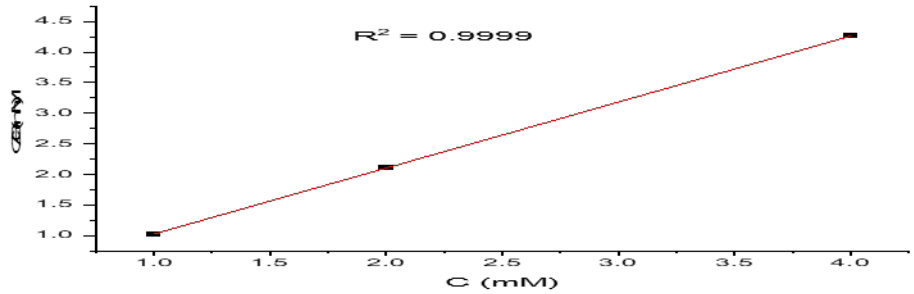


**Figure 6.** Langmuir isotherm plot for the adsorption of thiourea and Li ion on aluminium

**Thermodynamic Studies**

The relationship between adsorption equilibrium constant and free energy of adsorption ($\Delta G_{ads}$) during corrosion of metals at temperature dependent studies is stated in Eq (17 and 18) [22,23].

$$K_c = \frac{\theta}{C(1-\theta)} \quad (17)$$

$$\Delta G_{ads} = -RTIn(55.5K_c) \quad (18)$$

Where, 55.5 represents the water concentration ($MolL^{-1}$) and other parameters retain their standard meaning.

Generally, the value of $\Delta G_{ads}$ up to -20 $kJMol^{-1}$ is compatible with the physisorption, whereas those about –40 $kJMol^{-1}$ or higher values are related to chemisorption [24]. The computed $\Delta G_{ads}$ from the adsorption equilibrium constant ($K_c$) for thiourea and thiourea in combination with lithium ion ranged between -6.237 $kJMol^{-1}$ and -15.962 $kJMol^{-1}$ respectively. From the results obtained, we infer that the adsorption of the inhibitor molecules onto the aluminium substrate is physisorption and occurs spontaneously. The values of $\Delta G_{ads}$ confirm that the adsorption mechanism was by electrostatic interaction between the inhibitor molecules and charge on the aluminium surface [5,24].

The free energy of adsorption ($\Delta G_{ads}$) and adsorption equilibrium constant ($K_c$) values calculated are presented in Table 3. The link between the adsorbate and adsorbent is represented by $K_c$ Values. The increasing values of $K_c$ with an increase in temperature predict better inhibition efficiency. The negative value of the adsorption Gibbs free energy ($G_{ads}$) suggests that inhibitor molecules adsorb readily and permanently on the surface of an aluminum coupon, as well as the spontaneity of the corrosion inhibition process [25]. At all temperatures studied, the calculated value of $\Delta G_{ads}$ represents the physical adsorption of the inhibitor molecules on the metal surface [24]. The standard enthalpy ($\Delta H^o$) of adsorption and standard entropy ($\Delta S^o$) of adsorption were computed using Gibbs–Helmholtz equation as represented by Eq (19).

$$\Delta G^{\circ}_{ads} = \Delta H° - T\Delta S° \quad (19)$$

The variation of $\Delta G^{\circ}_{ads}$ against absolute temperature for aluminium corrosion in 3.5 % NaCl solution at different studied inhibitor was plotted in Figure 7a and b respectively. The values of enthalpy ($\Delta H^{\circ}_{ads}$) and entropy ($\Delta S^{\circ}_{ads}$) of the adsorption process were obtained from the intercept and slope of the linear plot, respectively, and presented in Table 3. The value of standard enthalpy of adsorption obtained in the systems studied is positive, thus suggesting an endothermic process ($\Delta H^{\circ}_{ads}$). As reflected in Table 3, the standard entropy of adsorption ($\Delta S^{\circ}_{ads}$) value obtained in the system is negative, which reflects the ordered manner of adsorption accompanied by free movement of inhibitor molecules in the bulk solution to the surface of the metal [5,22].

**Table 3:** Thermodynamic parameters for corrosion of aluminium in 3.5 % NaCl in the presence of thiourea and thiourea with lithium ion.

| Temp. (K) | $K_c$ | | $-\Delta G^{\circ}_{ads}$ (kJ/Mol) | | $+\Delta H^{\circ}_{ads}$ (kJ/Mol) | | $-\Delta S^{\circ}_{ads}$ (kJ/Mol) | |
|---|---|---|---|---|---|---|---|---|
| | Thiourea | Thiourea + lithium | Thiourea | Thiourea + lithium | Thiourea | Thiourea + lithium | Thiourea | Thiourea + lithium |
| 303 | 0.2143 | 0.3333 | 6.237 | 7.347 | | | | |
| 313 | 1.2857 | 1.7727 | 11.105 | 11.941 | | | | |
| 312 | 2.4412 | 2.4412 | 13.182 | 13.182 | 78.97 | 73.98 | 0.2841 | 0.2707 |
| 313 | 4.0455 | 5.7500 | 14.988 | 15.962 | | | | |

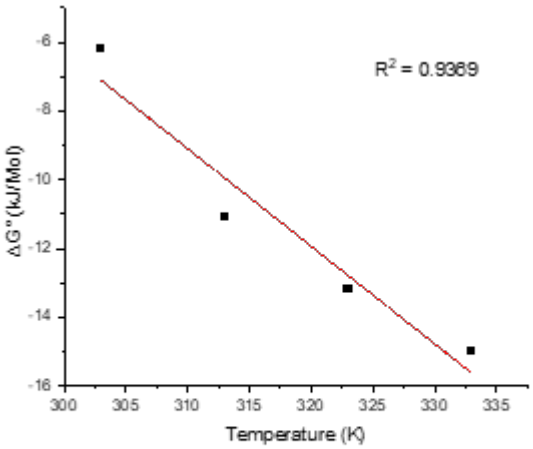


**Figure 7a:** Variation of ΔG against Temperature in 3.5 % NaCl on corrosion of aluminium in the presence of thiourea.

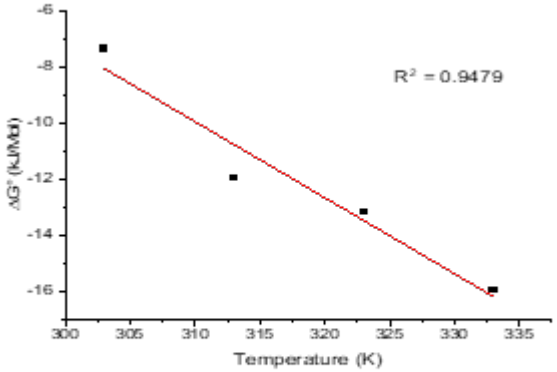


**Figure 7b:** Variation of ΔG against Temperature in 3.5 % NaCl on corrosion of aluminium in the presence of thiourea and lithium ion.

**Scanning Electron Microscopy (SEM) Analysis**

The SEM micrograph of the surface of the tested aluminium coupon was obtained in the absence and presence of inhibitor molecules studied after immersion in 3.5 % NaCl medium for 24 hrs at 303 K. Careful observation of Figure 8 reveals that the surface of the aluminium coupon in blank medium is very rough, corroded, and irregular as shown in Figure 8b. Figure 8c and d show that the morphology of aluminium coupons was smooth and rarely rough due to the adsorption of inhibitor molecules onto the aluminium surface. The added thiourea with the combination of lithium ions was able to cover almost all the cavities present on the surface, forming a barrier between the metal and the corroding medium, thereby preventing further corrosion.

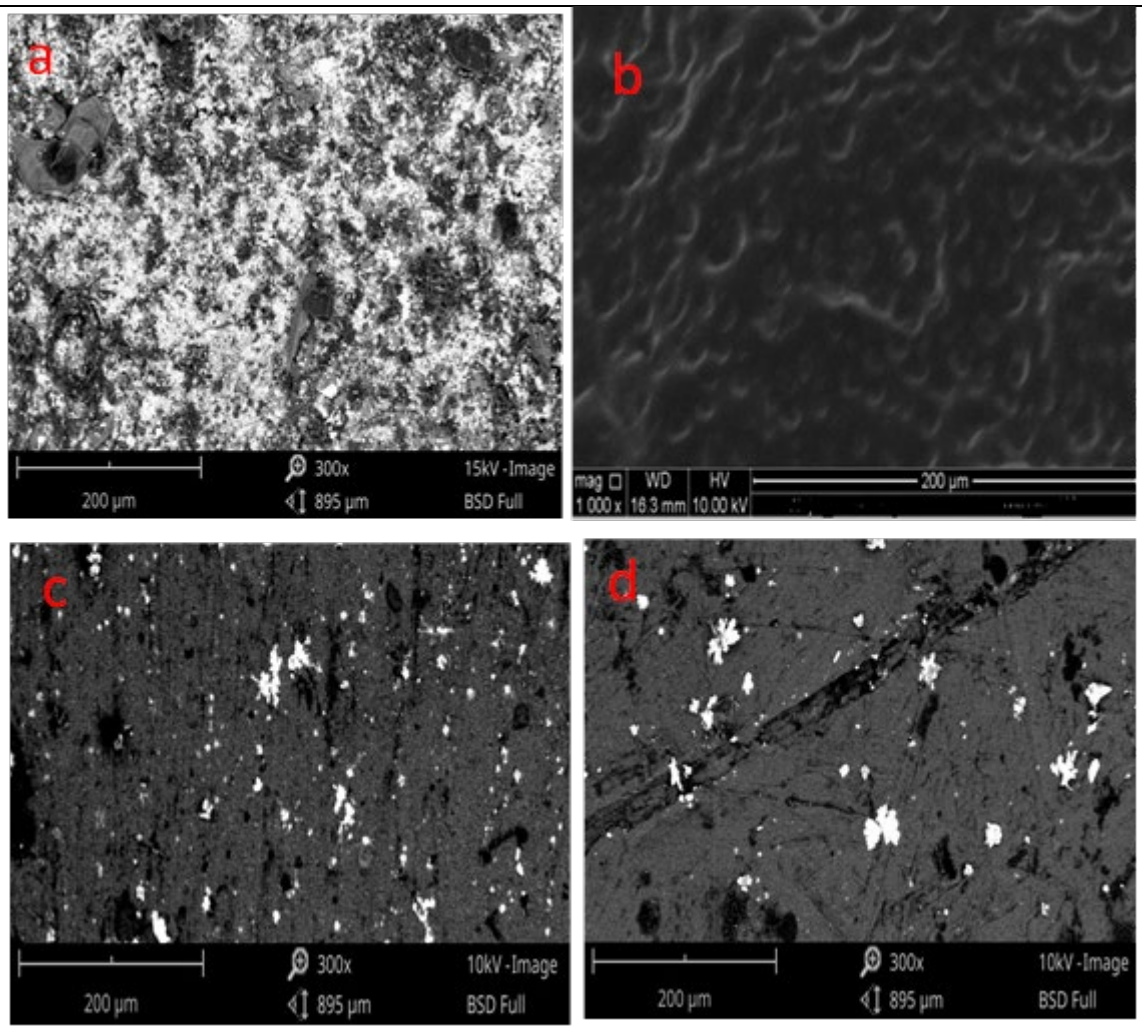


**Figure 8.** SEM micrograph of aluminium before immersion (a), after 24 h immersion in 3.5 % NaCl (b), after immersion with thiourea (c), after immersion with thiourea + Li ion (d).

**Quantum Chemical Computational Result**

**Chemical Reactivity of Inhibitor Molecules**

Quantum chemical theoretical calculations help to explore the electronic structure of molecules and provide an understanding of the relationship between molecular properties and their inhibition capability [26]. This optimized geometrical structure of the thiourea molecule, electron density, highest occupied molecular orbital (HOMO), and lowest unoccupied molecular orbital (LUMO) obtained from the simulation are shown in Figure 9. The thiourea molecule contains sulphur and nitrogen atoms. The electron density distribution is more concentrated on the $NH_2$ group. The energies of the frontier molecular orbitals ($E_{HOMO}$, $E_{LUMO}$, $\Delta E_{gap}$) obtained from the computational simulation were used to interpret the chemical reactivity of the inhibitive species and are -5.832 eV, -0.276 eV, and 5.556 eV respectively. Various quantum theoretical parameters for the thiourea are tabulated in Table 4. The HOMO and LUMO define the electron accepting and donating properties of the inhibitor, respectively. High values of $E_{HOMO}$ show the ability of the molecule to donate electrns to an appropriate acceptor like the unoccupied molecular orbital of the Al metal. The low value of $E_{LUMO}$ demonstrates electron take-up capability of the inhibitory molecule by the filled Al orbital. Hence, the high value of $E_{HOMO}$ decreased the value of $\Delta E_{gap}$ and the high value of $E_{LUMO}$ increased the value of $\Delta E_{gap}$. A low energy gap ($\Delta E_{gap}$) reduces the chemical reactivity of the inhibitor molecules, thereby, enhancing the interaction of the inhibitor molecules with the metal surface [27,28].

The superiority of inhibition can also be correlated to the value of the fraction of electrons transferred ($\Delta N$). This parameter is based on the absolute electronegativity of both the inhibitor and the metal and their absolute hardness [6]. The value of the fraction of electrons transferred ($\Delta N$) from inhibitor molecule to the metal surface is 0.458, which is less than 3.6. If $\Delta N$ is less than 3.6, the inhibitory effectiveness as a function of electron transfer of the molecules improves [29]. Furthermore, the low value of the global softness ($\sigma$) and the high value of the global hardness ($\eta$) supported the strong interaction between the Al metal and the inhibitor [30]. The absolute electronegativity ($\chi$) and global electrophilicity ($\omega$) of thiourea were 3.054 and 0.458, which also indicated the stability and reactivity of the inhibitor molecule.

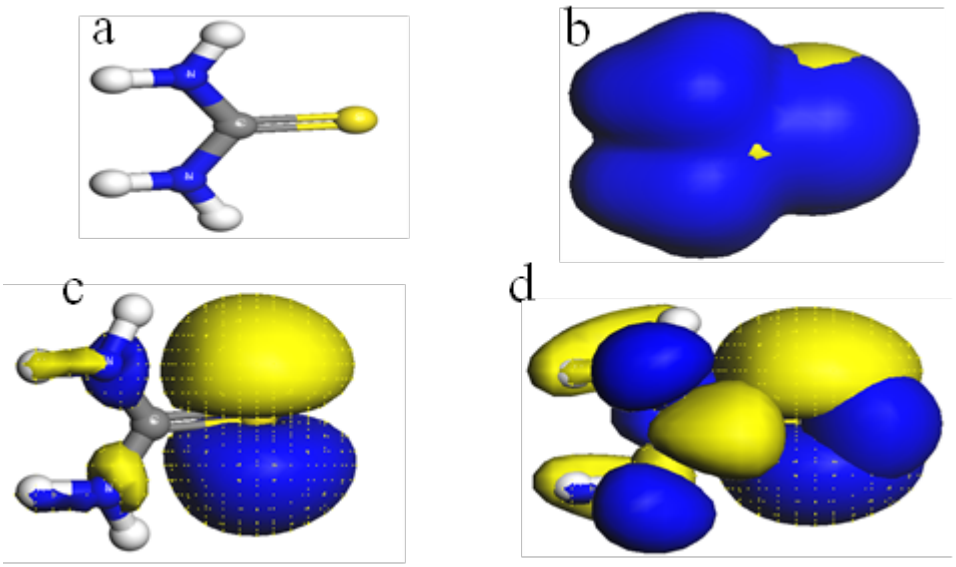


**Figure 9.** (a) Optimized structure, (b) Electron density around the optimized structure, (c) HOMO of the optimized structure, (d) LUMO of the optimized structure. Colour scheme: white = H, blue = N, yellow = Sulphur, grey = carbon.

**Table 4.** Quantum chemical parameters of thiourea

| Parameters | Values |
|---|---|
| HOMO (at orbital number) | 20 |
| LUMO (at orbital number) | 21 |
| $E_{HOMO}$ (eV) | -5.832 |
| $E_{LUMO}$ (eV) | -0.276 |
| Energy gap ($\Delta E_{gap}$) (eV) | 5.556 |
| Ionization potential (I) (eV) | 5.832 |
| Electron affinity (A) (eV) | 0.276 |
| Global hardness (η) | 2.778 |
| Global softness (σ) | 0.360 |
| Absolute electronegativity (χ) | 3.054 |
| Fraction of electron transfer (ΔN) | 0.458 |
| Global electrophilicity index (ω) | 1.679 |
| Global nucleophilicity (ε) | 0.596 |

**Fukui Functions**

The chemical reactivity of the thiourea molecule was analyzed using the Fukui function by indicating the sites for nucleophilic, electrophilic, and radical attacks on the molecule. These Fukui descriptors were calculated from natural populations for each atom in anionic, cationic, and neutral forms using the following equations:

$$f_k^+ = P_k(\mathrm{N+1}) - P_k(\mathrm{N}) \text{ for nucleophilic attack} \quad (20)$$

$$f_k^- = P_k(\mathrm{N}) - P_k(\mathrm{N-1}) \text{ for electrophilic attack} \quad (21)$$

$$f_k^0 = P_k(\mathrm{N+1}) - P_k(\mathrm{N-1}) \text{ for radical attack} \quad (22)$$

Where $P_k(\mathrm{N})$, $P_k(\mathrm{N+1})$ and $P_k(\mathrm{N-1})$ are the natural populations in the neutral, anionic and cationic for the atom k.

The concept of generalized philicity has been introduced in order to identify the philicity associated with a site k in a molecule with the corresponding condensed–to-atom variants of the fukui function [31]. Local electrophilicity ($\omega_k^+$and $\omega_k^-$) and local softness ($\sigma_k^+$ and $\sigma_k^-$) are both related to the nucleophilic and electrophilic attacks. The local electrophilicity ($\omega_k^\pm$) and softness ($\sigma_k^\pm$) can be calculated according to Eq 23 and 24 [32].

$$\omega_k^+ = \omega f_k^\pm \quad (23)$$

$$\sigma_k^\pm = \sigma f_k^\pm \quad (24)$$

Where $\sigma_k^+$ and $\sigma_k^-$ represent the local softness; and $\omega_k^+$and $\omega_k^-$ denotes the local electrophilicity for the nucleophilic and electrophilic attacks respectively. It has been affirmed that the dual local descriptors such as the difference between the nucleophilic and electrophilic fukui function ($\Delta f(k)$), the difference between the nucleophilic and electrophilic local softness ($\Delta\sigma_k$) and the difference between the nucleophilic and electrophilic philicity functions ($\Delta\omega_k$) are more accurate and consistent tools in measuring the local reactivity of corrosion inhibitors than the local reactivity indices [32-34]. The philicity indices $\Delta f(k)$, $\Delta\sigma_k$ and $\Delta\omega_k$ was calculated using equation 25 – 27.

$$\Delta f(k) = f_k^+ - f_k^- \quad (25)$$

$$\Delta\sigma_k = \sigma_k^+ + \sigma_k^- \quad (26)$$

$$\Delta\omega_k = \omega_k^+ - \omega_k^- \quad (27)$$

Table 5 shows the Fukui functions obtained from Milliken atomic charge for the atoms of thiourea molecule investigated. The favoured sites for the electrophilic attack are on atoms C1, N5 and N6. These atom sites could be electron acceptors. Thus, for the nucleophilic attack, the most reactive site is S4 atom. The sulphur atom shows an accumulation of excess negative charges on the molecule.

The HOMO orbital contains the sites for the electrophilic attack, which shows the region where the inhibitor molecule and metal surface exhibit the highest bonding ability. The LUMO orbital carries the site for nucleophilic attack, which represents the region where the inhibitor molecule and metal surface exhibit anti-bonding orbitals to form a feedback bond that strengthens the interaction between the inhibitor and aluminum surface [5]. In a thiourea molecule, the HOMO and LUMO orbitals respectively cut across the nitrogen and sulphur atoms within the molecule. Based on the obtained results, it can be concluded that the inhibitor highly adsorbs on the aluminum surfaces.

The results of the dual fukui function ($\Delta f_k$), dual local softness ($\Delta\sigma_k$), and dual local philicity ($\Delta\omega_k$) are summarized in Table 5. It has been reported that if the dual local descriptors ($\Delta f(k)$, $\Delta\sigma_k$, and $\Delta\omega_k$) values are less than zero, the adsorption process is favoured by electrophilic attack and nucleophilic attack is favoured if the local descriptors are greater than zero [35,36]. The dual local descriptors obtained in the present work (Table 5) show the most active sites (S4 and N5) for the local reactivity of the corrosion inhibitor. The dual local descriptor values suggest that S4 is the most active site for electron accepting centers and N5 is the most active site for electron donating centers for thiourea molecules, respectively. This indicates that S4 and N5 are the most preferred sites for corrosion inhibitor molecules to adsorb on the aluminium surface.

**Table 5.** Fukui Functions of Thiourea Molecules

| | C1 | S4 | N5 | N6 |
|---|---|---|---|---|
| P(N) | 0.100 | 0.554 | 0.065 | 0.064 |
| P(N+1) | 0.193 | 0.359 | 0.099 | 0.093 |
| P(N−1) | 0.006 | 0.749 | 0.030 | 0.035 |
| $f_k^+$ | 0.093 | −0.195 | 0.034 | 0.029 |
| $f_k^-$ | 0.094 | −0.195 | 0.035 | 0.029 |
| $f_k^0$ | 0.187 | −0.390 | 0.069 | 0.058 |
| $\sigma_k^+$ | 0.033 | −0.070 | 0.012 | 0.010 |
| $\sigma_k^-$ | 0.034 | −0.070 | 0.013 | 0.010 |
| $\omega_k^+$ | 0.156 | −0.327 | 0.057 | 0.049 |
| $\omega_k^-$ | 0.158 | −0.327 | 0.059 | 0.049 |
| $\Delta f(k)$ | −0.001 | 0.000 | −0.001 | 0.000 |
| $\Delta\sigma_k$ | −0.001 | 0.000 | −0.001 | 0.000 |
| $\Delta\omega_k$ | −0.002 | 0.000 | −0.002 | 0.000 |

**Molecular Dynamic Simulation (MDS) Results**

The adsorption behaviour of the inhibitor on aluminium was investigated using molecular dynamic simulation (MDS). Adsorption parameters for the interaction of thiourea molecules with Al(1 1 0) surface via forcite quench dynamics were determined in this study.

The interaction between energy ($E_{interaction}$) and binding energy ($E_{binding}$) was used to explain the interaction and adsorption capacity of studied inhibitor with the very fine surface of Al(1 1 0). Interaction energy and binding energy values are calculated according to the following relationship as shown in equations 28 and 29 respectively [36].

$$E_{interaction} = E_{total} - (E_{surface\ +solution} + E_{molecule}) \quad (28)$$

$$E_{binding} = -E_{interaction} \quad (29)$$

Where $E_{total}$ denotes the total energy of the whole system, $E_{surface\ +solution}$ represents the total energy of the metal surface and solution without the inhibitor molecule, and $E_{molecule}$ refers to the total energy of the inhibitor molecule. The adsorption properties of the inhibitor molecule and Al(1 1 0) surface such as kinetic energy, potential energy, energy of the inhibitor molecule, interaction energy and binding energy are presented in Table 6. Basically, it is assumed that the higher the negative adsorption value, the stronger the interaction between the adsorbent and adsorbate [37]. It has been reported that high interaction and binding energy values show the ability of the inhibitor molecule to displace the corrosive ions and $H_2O$ molecules from the aluminium surface to form a protective layer against the corrosive medium [38].

In this work, the calculated interaction energy value was −2468.075 kcal/mol, which shows the stability and spontaneous adsorption of the inhibitor onto the aluminium surface. The high positive value of binding energy (2468.075 kcal/mol) accounts for the good inhibition performance of thiourea. The large $E_{binding}$ obtained indicates that the corrosion inhibitor combines with the aluminium surface more easily and tightly via the physisorption process. The thermodynamic parameters were in agreement with the MDS results as they both agreed that the adsorption of inhibitor molecules on aluminium surfaces is through physical interaction.

Figure 10 depicts the snapshot of the stable configuration related to the lowest energy adsorption for the studied inhibitor molecule onto the surface of Al(1 1 0) at 350 K. It can be seen from the figure that thiourea molecules maintained a flat-lying adsorption orientation on the aluminium surface due to delocalization of the electron density around nitrogen and Sulphur atoms, which easily adsorbed on the aluminium surface [39].

**Table 6.** Values of adsorption parameters for the interaction of thiourea with the Al(110) surface using forcite quench dynamics.

| Molecule | Total kinetic energy (kcal/mol) | Total potential energy (kcal/mol) | Molecular energy (kcal/mol) | $E_{surface}$ (kcal/mol) | $E_{interaction}$ (kcal/mol) | $E_{binding}$ (kcal/mol) |
|---|---|---|---|---|---|---|
| Thiourea | 456.970 | −2573.075 | −105.015 | 0.000 | −2468.06 | 2468.06 |

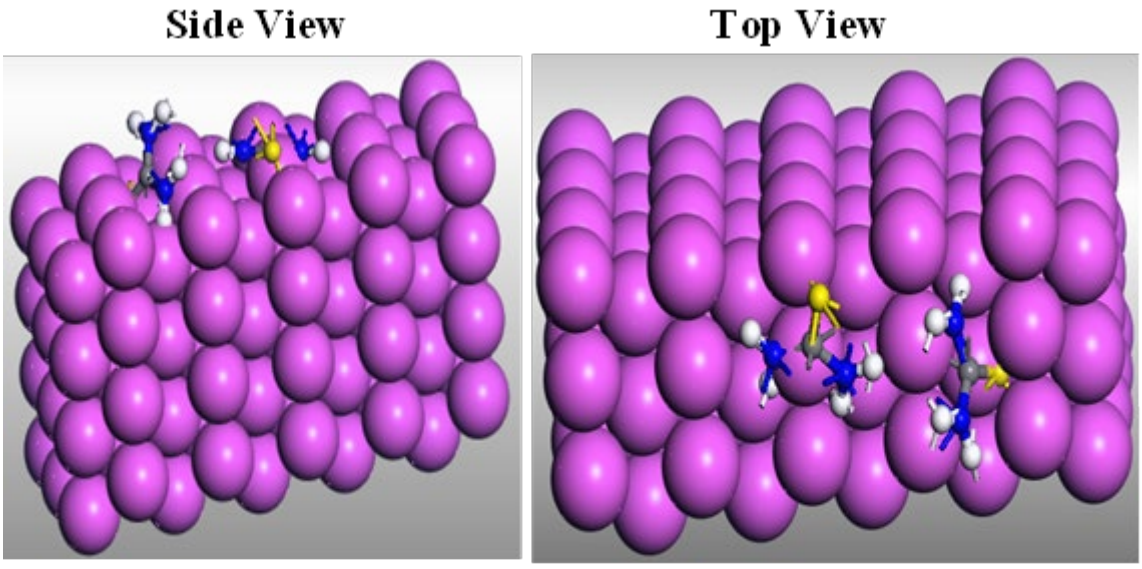


**Figure 10.** The stable adsorption configuration of thiourea molecule onto the Al(110) surface.

**Adsorption and Inhibition Mechanism**

The complex protective layer that regulates the rate at which metals collide in a corrosive environment occurs by displacement and adsorption. The chemical structure of the inhibitor, the charge on the molecule, the behavior of the corrosive medium, and the surface characteristics of the metal are the factors which affect the adsorption of the inhibitor onto the metal surface. Thiourea adsorbs onto the aluminum from aqueous solution, thereby suppressing $H_2$ pickup by blocking the active sites present on the metal, which are susceptible to corrosion. From the computational results of the thiourea inhibitor, the inhibitor shows the presence of electron density at the nitrogen atom, which helps in strong adsorption onto the aluminum surface by the formation of thin a film. The inhibiting atoms within the inhibitor molecule (sulphur and nitrogen) provide centers of adsorption which perform specific adsorption functions through either physical or chemical means. The interaction between aluminum and thiourea predominantly obeyed physisorption, as suggested by the thermodynamic parameters. Then, under the synergistic effect of thiourea and lithium ion, a self-assembled protective thin film can be formed very quickly on the aluminum surface. The inhibition mechanism with lithium-ion results from the formation of a protective film on aluminum surface during immersion and can occur according to the following steps: [40].

$$Al + 4OH^- \rightarrow Al(OH)_4^- + 3e^- \quad (30)$$

$$Al(OH)_4^- \rightarrow AlO_2^- + 2H_2O \quad (31)$$

$$Li^+ + AlO_2^- \rightarrow LiAlO_2 \quad (32)$$

However, the synergistic effect between thiourea and lithium ion forms a strong specific adsorption ability that is capable of covering both the cathodic and anodic areas on the aluminum surface. This explanation agrees with the observation of the results obtained in this work.

**Toxicity of Inhibitor**

The Absorption, Distribution, Metabolism, Excretion, and Toxicity (ADMET) properties were used to highlight the physical characteristics of the thiourea inhibitor and are summarized in Table 7. Carcinogenicity and mutagenicity were chosen to represent the toxicity of the inhibitor. The carcinogenicity and mutagenicity of the inhibitor were 0.5143 and 0.9600, respectively. Generally, predicted levels between 0.00 and 0.50 represent low toxicity probabilities,

while levels greater than 0.50 indicate high toxicity probabilities [32]. The $LD_{50}$ value of a toxic substance should be greater than 300 mg/kg. The acute toxicity of thiourea is 6260.82 mg/kg, which shows that the toxic level of thiourea is in a safe area [41]. The biodegradability of thiourea is 0.550, which shows that the inhibitor molecule is biodegradable and environmentally friendly.

**Table 7.** ADMET properties of thiourea

| ADMET properties | Values |
|---|---|
| Molecular weight | 76.12 g/mol |
| logP | −0.81 |
| H-Bond acceptor | 1 |
| H-Bond donor | 2 |
| Rotatable Bonds | 0 |
| Water solubility | 137.56 mg/kg |
| Acute oral toxicity | 6260.82 mg/kg |
| Biodegradability | 0.5500 |
| Water solubility (logS) | 0.2573 |
| Carcinogenicity | 0.5143 |
| Mutagenicity | 0.9600 |

## Conclusion

The inhibition behavior of thiourea and its synergistic effect with lithium ion for corrosion inhibition of aluminum in 3.5 % NaCl solution were investigated using gravimetric analysis, surface characterization techniques, and quantum chemical computational techniques. Based on the experimental findings, the results revealed that:

Thiourea is an effective corrosion inhibitor of aluminum in a NaCl environment. The corrosion inhibition efficiency decreases with increase in the concentration of the inhibitor.

The inhibition efficiency increases with the increase in the temperature of the NaCl solution.

The presence of lithium ion in the solution enhanced the inhibition efficiency of thiourea.

The synergistic effect of thiourea and lithium ion acted as a mixed indicator by covering both cathodic and anodic areas on the aluminum surfaces.

The corrosion process was controlled by the adsorption of the inhibitor molecules on the aluminum surfaces.

Adsorption of thiourea molecules on the examined metallic surface from corrosive media follows the Temkin isotherm model, while thiourea in synergistic effect with lithium ion follows the Langmuir isotherm model.

The adsorption of inhibitor molecules on the surface of aluminum involves physisorption based on the Gibb's free energy value.

The surface morphology study by SEM confirmed the adsorption of inhibitor molecules on the aluminum surface.

Quantum chemical calculations are in good agreement with the experimental results.

Thiourea molecules show significant corrosion protection properties and can emerge as an eco-friendly, green inhibitor with environmental and economic benefits. The major drawbacks are the mutagenicity and the concentration dependence of the percent inhibition efficiency of the tested inhibitor.

Further studies will be carried out to monitor the inhibitory effects of the studied compound on the aluminium surface in more detail using an electrochemical method.

**Funding:** Nigerian Tertiary Education Trust Fund (TETFund) through Institution Based Research (IBR) Project Grant (No. TETF/DR&D/CE/POLY/NEKEDE/IBR/2021/VOL.1).

**Acknowledgements:** The authors acknowledge TETFund for the financial support. We are also grateful to the staff of the Chemistry Department and Management of Federal Polytechnic Nekede, Owerri for providing the research facilities for this work.

Conflicts of Interest: The authors declare no conflict of interest.

## References

Gobara M., Baraka A., Akid R. and Zoraniy M. Corrosion protection mechanism of $Ce^{4+/}$organic inhibitor for AA2024 in 3.5 % NaCl. *RSC Advances*, 10, 2227-2240 (2020).

Liu W., An C., HaO J. and Li W. Cerium doped trimethoxy silane-aluminium isopropoxide coatings for enhanced corrosion protection of 1061 aluminium alloy in aqueous sodium chloride solution. *Int J. Electrochem. Sci.*, 16, 1-14 (2021).

Mohammadi I., Shahrabi T., Mohdavian M. and Izadi M. Cerium/diethldithiocarbamate complex as a novel corrosion inhibitive pigment for AA2024–T3. *Scientific Reports*, 10 5043 (2020).

Fajobi M.A., Loto T.R. and Oluwole O.O. Austenitic 316L stainless steel; corrosion and organic inhibitor: a review. *Key Engineering Materials*, 886 126-132 (2021).

Nwanonenyi S.C., Obasi H.C. and Eze 1.O. Hydroxypropyl Cellulose as an efficient corrosion inhibitor for aluminum in acidic environments. experimental and theoretical approach. *Chemistry Africa*, 1-11, (2019).

Shehu N.U., Gaya U.I. and Muhammad A.A. Influence of side chain on the inhibition of aluminium corrosion in HCl by $\alpha$−amino acids. *Applied Science and Engineering Progress*, 12, 3, 186 -197 (2019).

Ayuba A.M. and Abubakar M. Computational study for molecular properties of some of the isolated chemicals from leaves extract of *Guiera sengalensis* as aluminium corrosion inhibitor. *Journal of Science and Technology*, 13, 1, 47-56 (2021).

Ubaka K.G., Mong O.O. and Nleonu E.C. Investigation of inhibitory effect of thiourea on corrosion of mild steel in dual purpose Kerosene (DPK) and premium motor spirit (PMS). *International Journal of Advances in Engineering and Management*, 2,4, 162-168 (2020).

Yasakau K.A., Zheludkevich M.L. and Ferreira M.G.S. Role of intermetallics in corrosion of aluminium alloys smart corrosion protection. *Intermet. Matrix Compos*., 425-462 (2018).

Pais M. and Rao P. Electrochemical, spectroscopic and theoretical studies for acid corrosion of zinc using glycogen. *Chemical Papers*, 75, 1387-1399 (2021).

Li E., Wu J., Zhang D., Sun Y. and Chen J. D-phenylalanine inhibits the corrosion of Q235 carbon steel caused by

*Desulfovibrio sp*. *International Biodeterioration and Biodegradation*, 127, 178-184 (2018).

Al-Amiery A.A., Mohamad A.B., Kadhum A.A.H., Shaker L.M., Isahak W.N.R.W and Takriff M.S. Experimental and theoretical study on the corrosion inhibition of mild steel by nonanedioic acid derivative in hydrochloric acid solution. *Scientific Reports*, 12, 4705 (2022).

Jeslina V.D.A.M., Kirubavathy S.J., Al-Hashem A., Rajendran S.S., Joany R.M and Lacnjevac C. Inhibition of corrosion of mild steel by an alcoholic extract of a seaweed *Sargassum muticum*. *Zastita Materijala*. 6,2,4, 304-315 (2021).

Tan J., Guo L., Yang H., Zhang F. and El Bakri Y. Synergistic effect of potassium iodide and sodium dodecyl sulfonate on the corrosion inhibition of carbon steel in HCl medium: a combined experimental and theoretical investigation. *RSC Advances*, 10, 15163-15170 (2020).

Eddy N.O., Ameh P.O. and Essien N.B. Experimental and computational chemistry studies on the inhibition of aluminium and mild steel in 0.1 M HCl by 3-nitrobenzoic acid. *Journal of Taibah University for Science*, 12, 545-556 (2018).

Haldner R., Prasad D., Bahadur I., Dagdag O. and Berisha A. Evaluation of Gloriosa superba seeds extract as corrosion inhibition for low carbon steel in sulphuric acidic medium: a combined experimental and computational studies. *J. Mol. Lig.*, 323, 114958 (2020).

Mishra A., Verma C., Srivastava V., Lgaz H., Quraishi M.A., Ebenso E. E. and Chung M. Chemical, electrochemical and computational studies of newly synthesized novel and environmentally friendly heterocyclic compounds as corrosion inhibitors for mild steel in acidic medium. *Journal of Bio- and Tribo-Corrosion*, 4, 32 (2018).

Loto R.T., Loto C.A. and Popoola A.P.I. Corrosion inhibition of thiourea and thiadiazole derivatives: a review. *J. Mater. Environ. Sci.*, 3, 5, 885 – 894 (2012).

Al-Mosawi B.T.S., Sabri M.M. and Ahmed M.A. Synergistic Effect of ZnO nanoparticles with organic compound as corrosion inhibition. *International Journal of Low-Carbon Technologies*, 16, 429-435 (2021).

Nleonu E.C., Haldhar R., Ubaka K.G., Onyemenonu C.C., Ezeibe A.U., Okeke P.I., Mong O.O., Ichou H., Arrousse N., Kim S.C., Dagdag O., Ebenso E. and Taleb M. Theoretical study and adsorption behavior of urea on mild steel in automotive gas oil (AGO) medium. *Lubricants*, 10, 157, 1-13 (2022).

Oguzie E.E. Corrosion inhibitive effect and adsorption behavior of *Hibiscus sabdariffa* extract on mild steel in acidic media. *Port. Electrochem. Acta*., 26, 303-314 (2008).

Ezeibe A.U., Onyemenonu C.C., Nleonu E.C. and Onyema A.V. Corrosion inhibition performance of safranine towards mild steel in acidic corrosion. *International Journal of Scientific and Engineering Research*, 10, 5, 1539-1544 (2019).

Ezeibe A.U., Nleonu E.C. and Ahumonye A.M. Thermodynamics study of inhibitory action of lignin extract from *Gmelina arborea* on the corrosion of mild steel in dilute hydrochloric acid. *International Journal of Scientific Engineering and Research*, 7, 2, 133-136 (2019).

Nwanonenyi S.C., Obasi H.C., Oguzie E.E., Chukwujike I.C. and Anyiam C.K. Inhibition and adsorption of polyuinyl acetate (PVA) on the corrosion or aluminium in sulphuric and hydrochloric acid environment. *J. Bio Tribo Corros.*, 3, 53 (2017).

Mazkour A., El Hajjaji S., Labjar N., Lotfi E.M. and El Mahi M. Corrosion inhibition effect of 5-Azidomethyl-8-Hydroxyquinoline on AISI 321 stainless steel in phosphoric acid solution. *Int. J. Electrochem. Sci.*, 16, 1-24 (2021).

Mrani S.A., Arrousse N., Haldher R., Lahcen A.A., Amine A., Saffaj T., Kim S.C and Taleb M. In silico approaches for some sulfa drugs as eco-friendly corrosion inhibitors of iron in aqueous medium. *Lubricants*, 10, 43, 1-12 (2022).

Nazir U., Akher Z., Janjua N.K., Asghar M.A., Kanwal S., Butt T.M., Sani A., Liagat F., Hussani R. and Shah F.U. Biferrocenyl schiff bases as efficient corrosion inhibitors for an aluminium alloy in HCl solution: a combined experimental and theoretical study. *RSC Adv.*, 10, 7585-7599 (2020).

Arrousse N., Salim R., Kaddouri Y., Zarrouk A., Zahri D., El Hajjaji F., Touzani F., Taleb M. and Jodeh S. The inhibition behavior of two pyrimidine-pyrazole derivatives against corrosion in hydrochloric solution: experimental, surface analysis and in silico approach studies. *Arab. J. Chem.*, 13, 5949-5965 (2020).

Ayuba A.M., Uzairu A., Abba H. and Shallangwa G. A. Hydroxycarboxylic acids as corrosion inhibitors on aluminum metal: a computational study. *Journal of Materials and Environmental Sciences*, 9, 3026-3034 (2018a).

Abd El Wanees S. and Seda S.H. Corrosion inhibition of zinc in aqueous acidic media using a novel synthesized schiff base: an experimental and theoretical study. *J. Dispers Sci. Technol.*, 40, 1813-1826 (2019).

Parthasarathi R., Padmanabhan J., Elango M., Subramanian V. and Chattaraj P. Intermolecular reactivity through the generalized philicity concept. *Chem. Phys. Lett.*, 393, 225-230 (2004).

Cao K., Huang W., Huang X. and Pan J. Pyrimidine derivatives as effective inhibitor of mild steel corrosion in HCl solution: experimental and theoretical studies. *Front. Mater.*, 9, 843522 (2022).

Morell C., Grand A. and Toro-Labbe A. Theoretical support for using the $\Delta f(r)$ descriptor. *Chem. Phys. Lett.*, 425, 342-346 (2006).

Padmanabhan J., Parthasarathi R., Subramanian V. and Chattaraj P.K. Chemical reactivity indices for the complete series of chlorinated benzenes: solvent effect. *J. Phys. Chem. A.*, 110, 2739-2745 (2006).

Geerlings P., Ayers P.W., Toro-Labbe A., Chattaraj P.K. and De Proft F. The Woodward-Hoffmann rules reinterpreted by conceptual density functional theory. *Acc. Chem. Res.*, 45, 683-695 (2012).

Chen L., Lu D. and Zhang Y. Organic compounds as corrosion inhibitors for carbon steel in HCl solution: a comprehensive review. *Materials,* 15, 2023, 1-59 (2022).

Haldhar R., Kim S.-C., Prasad D., Bedair M., Bahadur I., Kaya S., Dagdag O and Guo L. *Papaver somniferum* as an efficient corrosion inhibitor for iron alloy in acidic

condition: DFT, MC simulation, LCMS and electrochemical studies. *J. Mol. Struct.*, 1242, 130822 (2021).

Guo L., Kaya S., Obot I.B., Zheng X. and Qiang Y. Toward understanding the anticorrosive mechanism of some thiourea derivatives for carbon steel corrosion: a combined DFT and molecular dynamics investigation. *J. Colloid Interf. Sci.*, 506, 478-485 (2017).

Hsissou R., Benhiba F., Dagdag O., El Bouchti M., Nouneh K. Assouag M. Development and potential performance of prepolymer in corrosion inhibition for carbon steel in 1.0 M HCl: outlooks from experimental and computational investigations. *J. Colloid Interf. Sci.*, 574, 43-60 (2020).

Rangel C.M. and Travassos M.A. Li-based conversion coatings on aluminium: an electrochemical study of coating formation and growth. Surf. Coatings Technol., 200, 5823-5828 (2006).

Alhaffer M.T., Umoren S.A., Obot I.B., Ali S.A. and Solomon M.M. Studies of the anticorrosion property of a newly synthesized green isoxazolidine for API 5L X60 steel in acid environment. *J. Mater. Res. Techn.*, 8, 4399-4416 (2019).